



Published in final edited form as:

Gene Ther. 2017 October ; 24(10): 610–620. doi:10.1038/gt.2017.54.

Recombinant elastin based nanoparticles for targeted gene therapy

Dagmara Anne Monfort¹ and Piyush Koria¹

¹Department of Chemical & Biomedical Engineering, University of South Florida, Tampa, FL 33620

Abstract

Among viruses, lentiviral vectors have been popular vectors for gene delivery due to their efficient mode of gene delivery. However, the non-specific delivery of genes associated with lentiviral vectors may result in undesirable side effects. Here, we propose a heterogeneous nanoparticle delivery system for targeted delivery of lentiviral particles containing a therapeutic gene. The heterogeneous nanoparticles consist of the low density lipoprotein receptor 3 (LDLR3) and the keratinocyte growth factor (KGF), each fused to elastin-like-polypeptides (ELPs), LDLR3-ELP and KGF-ELP, respectively. Our results show that while homogeneous nanoparticles comprising of LDLR3-ELP alone blocked viral transduction, heterogeneous nanoparticles comprising of KGF-ELP and LDLR3-ELP enhanced viral transduction in cells expressing high levels of the KGF receptors compared to cells expressing low levels of KGF receptors. Overall, this novel design may help with the targeting of specific cells that overexpressed growth factor such as KGF receptors.

Keywords

Fusion proteins; KGF; transduction; drug delivery; lentiviral vector; VSV-G; LDLR; nanoparticles

INTRODUCTION

Genetic diseases caused by a defective gene, single modification in a gene or mutations affect millions of people worldwide. People with genetic diseases such as cystic fibrosis (1), cancer (2), and Parkinson's (3) are getting treatments to improve their quality of life but there are no cures for these diseases. Gene therapy that aims to deliver a gene of interest to replace, inactivate or correct the defective gene to help the diseased tissue function properly is the most promising approach for curing these debilitating genetic diseases. Scientists have used multiple gene delivery techniques such as lipid mediated gene delivery (4), cationic polymers (5), electroporation (6), microinjection (7), and viruses (8). Due to their efficient

Users may view, print, copy, and download text and data-mine the content in such documents, for the purposes of academic research, subject always to the full Conditions of use: http://www.nature.com/authors/editorial_policies/license.html#terms

*Address for all correspondence: Piyush Koria, Department of Chemical & Biomedical Engineering, 4202 E Fowler Avenue, ENB 118, Tampa, FL 33620, Tel: 813-974-6243, pkoria@usf.edu.

COMPLIANCE WITH ETHICAL STANDARDS

Conflict of interest: The authors declare that they have no conflict of interest.

mode of gene delivery, viruses such as lentivirus are popular vectors for gene delivery (9). Lentiviral vectors are attractive because they can infect both dividing and non-dividing cells (10–12), and they integrate into the cells' genome (13). The problem with lentiviral vectors is their lack of specificity, which can result in indiscriminate transduction (14). The non-specific delivery of therapeutic genes could lead to undesirable side effects such as toxicity (15, 16), insertional mutagenesis (15, 16), and immunogenicity (15, 16). The need for targeted therapy is imperative because it could lower the probability of these undesirable side effects and increase the probability of delivering the gene of interest to the desired site.

Most recombinant lentiviral vectors in use for gene therapy are pseudotyped by the vesicular stomatitis virus (VSV) glycoprotein G (VSV-G) (17). This is primarily due to VSV exhibiting a very robust and pantropic infectivity which has been extensively studied and characterized (18). VSV-G pseudotyped lentiviruses display remarkable stability, high transduction efficiency and the same broad tropism as VSV. Thus, currently they are the gold standard for several gene therapy procedures (19). Recent studies have indicated that VSV-G interacts with the low density lipoprotein receptor (LDLR) thereby enabling the entry of the virus into the cells (20). The widespread expression of LDLR accounts for the broad applicability of VSV-G pseudotyped viral vectors for gene therapy.

Elastin like polypeptides (ELPs) are gaining popularity as drug delivery vectors (21, 22) due to their ability to be genetically encodable and to undergo phase transition (23). ELPs are protein-based polymers that have been used as novel drug carriers (24–26). They are composed of repeating sequence of pentapeptides, $(\text{Val-Pro-Gly-X-Gly})_n$ where X can be any amino acids except for Proline (27). Proline destroys the inverse phase transition property of ELPs (28). This sequence of pentapeptides is derived from the hydrophobic chain of tropoelastin, a soluble form of elastin (29). ELPs have an interesting physical property where they undergo an entropically driven phase transition rendering them insoluble above the transition temperature (29). This property enables ELPs to be expressed in a bacterial host (such as *Escherichia coli*) and to be purified rapidly using inverse temperature cycling (ITC) (30). Moreover, since ELPs are genetically encodable, chimeric fusion proteins comprising of biologically active motifs and ELPs can be synthesized easily (31, 32). These fusion proteins retain the biological activity of the fused motif as well as the phase transitioning property of ELPs, thereby enabling the self-assembly of nanostructures such as nanoparticles above the transition temperature (32). These characteristics of ELPs make them attractive targeted delivery vehicles for viral gene delivery.

Our lab has previously described a heterogeneous nanoparticle delivery system based on ELPs that focuses on selective delivery of peptides through selective enhancement of macropinocytosis via growth factors (33). Here we describe the application of the same delivery system for targeted delivery of lentiviral particles to high growth factor receptor expressing cells. Specifically, we report the construction of heterogeneous nanoparticles comprising of two chimeric ELP fusion proteins, namely the low density lipoprotein receptor repeat 3 (LDLR3)-ELP and keratinocyte growth factor (KGF)-ELP. We report that VSV-G pseudotyped lentiviral particles bind to the heterogeneous nanoparticles via LDLR3-ELP, thereby preventing viral entry in cells. We further show that the heterogeneous nanoparticles containing the bound lentiviral vector are internalized in cells overexpressing

the keratinocyte growth factor receptor (KGFR) via KGF-ELP, thereby resulting in successful targeted transduction. We believe that this approach of selective transduction will lead to successful gene therapy treatment with minimum side effects. Moreover, the modular nature of the chimeric ELP fusion protein system ensures that this approach can easily be used to target any growth factor receptor thereby broadening the applicability of this strategy to multiple cell types.

RESULTS

Fusion Protein Comprising of the Viral Envelope Binding Domain (VBD) and Elastin Like Polypeptide (ELP) was Successfully Expressed and Purified Using Inverse Temperature Cycling (ITC)

Previous studies have shown that virus pseudotyped with the vesicular stomatitis virus glycoprotein G (VSV-G) envelope enters the cell by binding with the low density lipoprotein (LDL) receptor (20). In order to create a fusion protein that binds to the lentiviral vector to prevent the non-selective infection of untargeted cell types, a fragment of the LDL receptor gene, LDL receptor repeat 3 (LDLR3), was cloned upstream of the elastin like peptide gene (Figure 1A).

This gene encoding the fusion protein LDLR3-ELP (where ELP is V40C2) was then expressed in a bacterial host (*E. coli*) and purified by ITC. After three ITC cycles, isolated protein was stained with simply safe blue and analyzed for purity by SDS-PAGE gel electrophoresis. The single black band with a molecular weight of 50 kDA shown in figure 1B confirms purity of LDLR3-ELP fusion protein.

LDLR3-ELP Maintains the Phase Transition Property and Self Assembles Into Nanoparticles

The successful purification of LDLR3-ELP using ITC suggests that LDLR3-ELP fusion protein retained the physical phase transition property characteristic of ELPs. To further characterize the phase transitioning property of LDLR3-ELP, dynamic light scattering (DLS) was used to analyze the transition temperature of LDLR3-ELP at a concentration of 2 μ M. The results show that LDLR3-ELP transitions near 30°C (Figure 2A). Previous studies described for other ELP based fusion proteins (27) state that at the transition temperature the fusion protein form fairly monodispersed aggregates with radii in the nanometer range. To ascertain whether this is the case with LDLR3-ELP, we measured the particle size and dispersity with DLS at a concentration of 2 μ M, at homeostatic physiological temperature 37°C. The dispersity of proteins was tightly distributed around a mean size of 150 nm with respective minimum and maximum sizes of 12 nm and 615 nm with 96.4% of peak 1 area intensity is 204 nm and 3.6% of peak 2 area intensity is 3.6 nm (Figure 2B).

LDLR3-ELP Inhibits Lentivirus Infectivity and does not Induce Cell Death

Previous studies have shown that recombinant soluble LDLR (sLDLR) inhibited transduction by a lentivirus pseudotyped with the VSV-G envelope (20). To test if LDLR3-ELP fusion protein maintained the activity of the fused LDLR3 domain, a transduction assay using lentiviral particles pseudotyped with the VSVG envelope containing the green

fluorescent protein (GFP) gene was performed. The lentivirus and LDLR3-ELP fusion protein were incubated together and then introduced to cells. Indeed, 20 μM of LDLR3-ELP inhibited the viral transduction efficiency of more than 99% (Figures 3A and 3B).

Previous studies have reported that sLDLR inhibits virus infectivity by binding to the VSV-G envelope of the lentivirus. To show that the LDLR3-ELP binds with the lentivirus pseudotyped with VSV-G envelope, we incubated the lentiviral vector with different concentrations of LDLR3-ELP fusion protein. The transitioned LDLR-3-ELP along with any bound lentiviral vector was then pelleted by centrifugation and the supernatant was collected. The collected supernatant was then put atop of the cells and flow cytometry was used to quantify the data. Indeed, we observed a decrease in transduction efficiency of more than 90%. This suggests that most of the lentiviral vector was bound to the LDLR-3-ELP (Figures 4A and 4B). We also carried out an immunoprecipitation assay using magnetic beads to show lentiviral vector binding to LDLR3-ELP at 4°C or 37°C (Figure 4C). Interestingly, the binding increased by nearly 3 folds at 37°C compared to 4°C and thus we carried out the viral binding at 37°C for subsequent experiments.

We further performed an MTT assay to make sure that LDLR3-ELP was not toxic to cells. Our results indicate that LDLR3-ELP with a concentration as high as 20 μM is not toxic to cells (Figure 5).

Targeted Internalization of LDLR3-ELP Using Growth Factors in High Growth Factor Receptor Expressing Cells

Our results clearly indicate that LDLR3-ELP binds to the lentiviral vector and thus prevents the lentiviral vector from entering and infecting the cells. We reasoned that the lentivirus can selectively be delivered to the cells by targeted delivery of LDLR3-ELP to the cells. We have previously described a heterogeneous ELP based nanoparticle delivery platform containing growth factors that selectively delivers payload in high growth factor receptor expressing cells. We reasoned that targeted gene therapy can be achieved using this platform (33). To test this hypothesis we created heterogeneous nanoparticles (NPs) comprising of keratinocyte growth factor (KGF)-ELP and LDLR3-ELP (Figure 6A). To test if KGF-ELP enhances the internalization of LDLR3-ELP, heterogeneous nanoparticles containing labeled LDLR3-ELP and KGF-ELP were created. Indeed, these heterogeneous NPs were selectively internalized and able to deliver LDLR-3-ELP in the high KGFR expressing A549 cells (Figure 6B).

Heterogeneous Nanoparticles Comprising of LDLR3-ELP and KGF-ELP Result in Targeted Delivery of the Gene in High Growth Factor Receptor Expressing Cells

Next, we tested whether the heterogeneous NPs comprised of LDLR-3 ELP and KGF-ELP can selectively deliver the VSV-G pseudotyped lentiviral vector to high KGFR expressing A549 cells, thereby resulting in selective transduction. To this end, the lentiviral vector was incubated with 1 μM LDLR3-ELP and the LDLR3-ELP bound with the lentiviral vector was collected by centrifugation. The pellet containing the LDLR-3-ELP bound with the lentiviral vector was re-suspended in cold media and was then mixed with 1 μM KGF-ELP, resulting in the formation of heterogeneous NPs containing the lentiviral vector and KGF-ELP. These

heterogeneous nanoparticles have a higher probability of being uptaken by high KGFR expressing cells (A549 cells) than low KGFR expressing cells (H293 cells) (Figure 7A). These nanoparticles resulted in a 5.5 fold increase of transduction efficiency in high KGFR expressing A549 cells. (Figure 7B). On the other hand there was a modest increase of about 1.5 fold in H293 cells which have low levels of the KGFR (Figure 7B). To determine the number of gene copies per cell we quantified the geometric mean of the fluorescence intensity of each treatment. These intensities were normalized to the corresponding control cell types to account for the variability of transduction due to cell types. We found that there was a 30 % increase in the normalized intensity in A549 cells compared to H293 cells (Figure 7C) suggesting that multiple viral particles were introduced in the high KGFR expressing A549 cells line.

As described previously in our lab the heterogeneous nanoparticles are selectively delivered in high KGFR expressing cell lines via KGF induced macropinocytosis (33). To further show that this is indeed the case here, we carried out the experiments in the presence of recombinant KGF (rKGF). Indeed, rKGF enhanced the transduction efficiency in both homogeneous LDLR3-ELP nanoparticles as well as in LDLR3-ELP and KGF-ELP heterogeneous nanoparticles (Figure 8).

ELP and KGF-ELP do not bind to the Virus

To confirm that the increase in transduction efficiency demonstrated by the heterogeneous NPs is not because of KGF binding with the lentiviral vector, we tested whether KGF-ELP or ELP binds to the lentiviral vector. The lentiviral vector with either 12 μ M ELP or 12 μ M KGF-ELP were incubated together and centrifuged. Cells were then treated with the supernatant and the transduction efficiency was assessed. Indeed, neither the ELP nor the KGF-ELP treatment of the lentiviral vector resulted in a decrease in transduction efficiency of the viral supernatant (Figures 9A and 9B) thus suggesting that neither of them bound to the virus.

Virus is Released from LDLR3-ELP after Cellular Internalization

To test if the virus remained bound to LDLR-3-ELP after cellular entry we carried out immunoprecipitation assay of cell lysates treated with the lentiviral vector containing heterogeneous NPs. We found that the lentiviral vector was released from the LDLR3-ELP nanoparticles within 24 hours of treatment (Figure 10). These data suggest that after internalization of the virus containing nanoparticles, the lentiviral vector detaches itself from LDLR3-ELP.

DISCUSSION

Gene therapy is a promising technique for the treatment of many debilitating genetic diseases, such as cystic fibrosis and cancer. Targeted gene therapy is essential because it may lower the probability of side effects including toxicity (15, 16), insertional mutagenesis (15, 16), and immunogenicity (15, 16). Viruses, such as lentiviruses, are attractive options for gene therapy because they can integrate into the cells' genome (13) and infect both dividing and non-dividing cells (10–12). Here, we described a novel approach that results in the

selective internalization of the lentiviral vector encoding a GFP gene in cells that overexpress keratinocyte growth factor receptors, thereby delivering the gene to the targeted cells. Specifically, we created heterogeneous nanoparticles comprising of two chimeric fusion proteins namely, low density lipoprotein receptor 3 (LDLR3)-ELP and keratinocyte growth factor (KGF)-ELP. We show that the heterogeneous nanoparticles deliver the lentiviral vector selectively to high KGF receptor expressing cells resulting in selective delivery of the gene encoding green fluorescent protein to those cells.

Important characteristics of ELP include: they can undergo self-assembly at a transition temperature, they are genetically encodable, immunogenic; and they are biocompatible. We demonstrated that the fusion protein, LDLR3-ELP, maintained the phase transition property and self-assembled into nanoparticles above transition temperature. These fusion proteins retained the biological activity and phase transitioning properties of ELPs, as shown in previous studies (29, 31, 32). This allowed recombinant expression and simple purification of the fusion proteins by a series of hot and cold cycles. Self-assembly is important because this quality allows for the creation of chimeric nanoparticles comprising of different chimeric fusion proteins such as KGF-ELP and LDLR3-ELP as described here. Additionally, synthetic genes encoding any ELP fusion proteins can easily be synthesized using standard molecular biology approaches. Thus, this approach can easily be broadened to include other growth factors to target other cells expressing different growth factor receptors such as epidermal growth factor receptor (EGFR) or nerve growth factor receptor (NGFR).

Our experiments indicate that LDLR3-ELP inhibited transduction by a lentivirus pseudotyped with the vesicular stomatitis virus glycoprotein G (VSV-G) envelope. We further demonstrated that this inhibition was mediated by the binding of the LDLR3-ELP to the lentiviral vector. This inhibition is similar to previous studies that have shown that recombinant soluble LDLR (sLDLR) inhibited transduction by a lentivirus pseudotyped with the VSV-G envelope (20). This study further demonstrated that the inhibition was mediated by the binding of the sLDLR to the VSVG envelope, thereby preventing the lentiviral vector from binding to the LDL receptor on the target cells and denying its entry. We believe that LDLR3-ELP blocks the viral transduction in a similar fashion. The binding of the LDLR3-ELP to the lentiviral vector indicates that the binding ability of LDLR3, in the fusion protein LDLR3-ELP, remained unaffected. This observation is similar to previous studies by several others and us for chimeric ELP fusion proteins where the biological activity of the functional domain remains unaffected by the ELP fusion (31, 32). Moreover, the inhibitory activity of LDLR3-ELP without KGF-ELP also demonstrates that its potential application as an agent in antiviral therapy.

Viruses can infect multiple cells causing undesired side effects. Thus, to minimize side effects, it is essential to selectively deliver the virus only to the target cells. We further show that heterogeneous nanoparticles comprising of LDLR3-ELP and KGF-ELP can induce selective transduction of VSV-G pseudotyped lentiviral vector in high KGFR expressing cells. This can be explained by enhanced internalization of the lentiviral vector mediated by the heterogeneous nanoparticles. Interestingly, we observed that the transduction efficiency induced by the heterogeneous nanoparticles was further increased by recombinant KGF.

This indicates that the selective internalization is not a receptor mediated internalization process. On the contrary we believe that the internalization of the lentiviral vector bound to LDLR-3-ELP is mediated by KGF induced macropinocytosis which has been previously described in our lab (33).

While several nanoparticulate systems have been developed for the targeted delivery of plasmids (34) or SiRNA (35), very few studies focus on the selective delivery of viruses for targeted gene therapy. For example, the use of magnetic nanoparticles loaded with adenoviral vectors for gene delivery to stented arteries has been described (36). It is to be noted that a magnetic field was used to achieve site specific delivery in that approach. A similar approach involving magnetic nanoparticles and lentivirus has been described for the transduction of endothelial cells (37) and the delivery of oncolytic adenovirus (38). Nonetheless, the targeted approach described in this work is different than these strategies as it focuses on the ligand receptor interactions as opposed to providing a magnetic field for site specific delivery. Moreover, applying site directed magnetic field in various parts of the body could be challenging as opposed to simply targeting the receptors for gene delivery.

It is to be noted that here we have employed a single cysteine-rich repeat (No. 3) of the LDLR fused with ELP and expressed in *E. Coli* for binding of the lentiviral vector. The LDL-binding region of LDLR consists of 7 cysteine-rich repeats and needs to be expressed in eukaryotes in order to maintain correct folding and correct disulfide bonding. Consequently, the binding affinity of the LDLR3-ELP to the viral vector is very low, requiring 20 μM or 1.5 mg/ml of nanoparticles to inhibit the viral vector (Figure 3). This concentration translates to at least 10 g of nanoparticles per 6 L of the blood of one patient. This amount is far from being practical and thus fusion proteins having higher binding affinity need to be generated in the future, for successful in vivo experiments and translation to clinic. Nonetheless the approach is promising ex-vivo and currently we are working on developing novel fusion proteins with higher binding affinities.

In summary, we have developed a novel nanoparticle based delivery system for targeted delivery of the VSV-G pseudotyped lentiviral vector encoding a green fluorescent protein gene to cells. Delivering the lentiviral vector to the target cells selectively has been a major challenge. We demonstrated that the chimeric ELP fusion protein heterogeneous NPs consisting of LDLR3-ELP as a viral binding domain and KGF-ELP as a targeted protein, can overcome this challenge. This novel design may help target specific cells and can be used as an application for treatment of genetic diseases while limiting side effects of non-targeted gene delivery.

MATERIALS AND METHODS

Materials

Dulbecco modified eagle medium (DMEM) and fetal bovine serum (FBS) were purchased from Life Technologies. A549, H1650, H23, and H292 cells were kindly donated by Dr. Haura from Moffit Cancer Center. Peptide genes and growth factors were purchased from GenScript (Piscataway, NJ). H293 cells were purchased from ATCC (Manassas, VA). The gel extraction, miniprep, and midiprep kits were purchased from QIAGEN (Valencia, CA).

RT-PCR reagents were purchased from Bio-Rad (Hercules, CA). The restriction enzymes and other enzymes used for cloning were purchases from New England Biolabs (Ipswich, MA). The lentiviral plasmids: psPAX2 and pMD2.G was a gift from Didier Trono (Addgene plasmid #12259 and #12260, respectively). The lentiviral gene plasmid, pLVTHM-syndecan-1 shRNA GFP, was kindly donated by Dr. Ralph Sanderson from University of Alabama.

Cell Culture

Human lung carcinoma cells, A549 and H292, and human lung adenocarcinoma cells, H23 and H1650, and human embryonic kidney cells, H293, were cultured in DMEM supplemented with 10% FBS and 1% antibiotic antimycotic (AA) in a humidified incubator at 37°C and 5% CO₂.

Synthesis of LDLR3-ELP and KGF-ELP

The pUC57 plasmids containing the genes (VPGVG)₂VPGCG(VPGVG)₂, LDLR3, and KGF were purchased from GenScript (Piscataway, NJ). Recursive direction ligation method was used to create V40C2 encoding gene as previously described (39). PflMI and BglI enzymes were used to cut the LDLR3 and KGF genes. A 1.0% agarose gel was used to run these genes. The genes were then extracted using QIAquick gel extraction kit. The PflMI was used to linearize the pUC19 vector containing the ELP sequence and the removed LDLR3 or KGF genes were cloned in with the ELP gene. As a result, the pUC19 vector containing LDLR3-ELP or the KGF-ELP fusion protein gene situated by PflMI and BglI sites. PflMI and BglI enzymes were used to remove the sequence encoding fusion proteins from the pUC19 vector. As mentioned above, a gel extraction was performed to recover the sequence encoding fusion proteins. The pET25b+ expression vector was modified to incorporate a SfiI cloning site for the LDLR3-ELP or the KGF-ELP fusion protein gene to be cloned. Through heat shock at 42°C, the pET25b+ expression vector containing the LDLR3-ELP or the KGF-ELP fusion protein gene was transformed into BLRD competent cells.

Purification of LDLR3-ELP

For protein production, the BLRD competent cells were grown overnight in an agar plate. A single colony was selected from the streaked agar plate containing carbenicillin for starting a culture of 75 mL. This culture was inoculated overnight and transferred to a one liter culture the next day. This one liter culture was grown overnight and inverse transition cycling was used to purify LDLR3-ELP or the KGF-ELP fusion as previously described (27). Since LDLR3-ELP have six cysteine residues, double amount of the reducing agent dithiothreitol (DTT) was added to the cold centrifugation to reduce the formation of disulfide bonds. After the ITC process, the ELP fusion proteins solution were dialyzed for 48 hours. They were then lyophilized for 72 hours to be stored at room temperature.

LDLR3-ELP Total Protein Assay

The fusion protein LDLR3-ELP purity was conducted using total protein stain assay with sodium dodecyl sulfate polyacrylamide gel electrophoresis (SDS-PAGE). The lyophilized

LDLR3-ELP was dissolved in 4°C PBS to a final concentration of 2 µM and 10 µM. Both the bacterial lysates and the dissolved lyophilized LDLR3-ELP were analyzed by SDS-PAGE (12% acrylamide gels).

Characterization of LDLR3-ELP

Dynamic light scattering (DLS) instrument (Zetasizer Nano S, Malver, UK) was used to analyze the transition temperature from 4°C to 40°C at a step of 2°C and size of the LDLR3-ELP at the body's physiological temperature, 37°C. Three readings were performed in each temperature point with an equilibrium time of 10 minutes. For both transition temperature and size, 2 µM of LDLR3-ELP was prepared in 1X phosphate buffered saline (PBS) and 1 mL of the solution was inserted into a cuvette for readings. For the transition temperature, readings were based on scattered light intensity versus temperature. For the size, readings were based on mean intensity versus diameter size at 37°C.

Labeling of the Fusion Proteins

For the particle internalization experiments, fluorescein-5-maleimide (AnaSpec Inc cat # 81405) was used to label the cysteines that are present in the fusion proteins. Fluorescein-5-maleimide was added to the fusion proteins. The mixture was incubated at room temperature for one hour on an orbital shaker. Then it was incubated at 4°C overnight. A series of hot and cold cycles were then performed to remove unconjugated fluorescein on a centrifuge at 20,000 G for 10 minutes each time. After the hot spin, the supernatant was discarded and equal amount of volume of cold sterile PBS was added. Once the pellet was dissolved, the supernatant was collected at 4°C. The hot and cold cycle was repeated at least two times to remove all of the unconjugated fluorescein.

For the immunoprecipitation assay, LDLR3-ELP was conjugated with biotin-maleimide (Sigma-Aldrich cat # B1267). The above protocol was applied to remove unconjugated biotin.

Internalization assay for fusion proteins

Cells (20,000/well) were seeded in a 48-wells plate and cultured in DMEM supplemented with 10% FBS and 1% AA. They were grown until 30% confluency is reach and were starved for 24 hours then were treated in serum free media with the indicated treatments for 48 hours. Lentiviral vectors were not added in this experiment. For analysis, plate was put on ice for five minutes to dissolve fusion proteins, then cells were wash three times with ice-cold sterile PBS and were trypsinized using 0.25% trypsin (200 uL). The trypsin reaction was neutralized by an addition of 200 uL of DMEM supplemented with 10% FBS and 1% AA. Solution were transferred into micro-test tubes and cells were pelleted and re-suspend in 250 µL of PBS containing 50 µg/mL of trypan blue to capture only the internalized labeled fusion proteins and not the ones that are bound to the periphery of the cells. Flow cytometry was used to quantify the data and the percent of fluorescent cells was reported.

Cytotoxicity Assay

Cells (20,000/well) were seeded in a 48-wells plate and cultured in DMEM supplemented with 10% FBS and 1% AA. They were grown until 30% confluency is reached and were

starved for 24 hours then were treated in serum free media with the indicated treatments for 48 hours. After their respective treatments, plate was put on ice for five minutes to dissolve fusion proteins, then cells were wash three times with ice-cold sterile PBS. Thiazolyl blue tetrazolium bromide (MTT, Acros Organics cat # 298-93 uL) was added to each well to a final concentration of 1.2 mM. Cells were then incubated for three hours at 37°C. After the incubation time, cells were washed once with room temperature sterile PBS to remove the excess MTT medium. Dimethyl sulfoxide (DMSO, Fisher Bioreagents cat # BP231-1) was added to solubilize the formazan crystals. For data analysis, EON microplate spectrophotometer (BioTek, Winooski, VT) was used to read the absorbance at 570 nm.

Transduction Assay

A549 cells (20,000/well) and H293 cells (30,000/well) were seeded in a 48-wells plate and cultured in in DMEM supplemented with 10% FBS and 1% AA, respectively. A549 were grown until 30% confluency is reached and were starved for 24 hours, whereas H293 cells were cultured with 10% FBS throughout the experiment. H293 cells treatment started when their confluency reached 30%. LDLR3-ELP was added to the lentivirus and the micro-test tubes were incubated at 4°C for 15 minutes. Afterwards, all vials were incubated at 37°C for 30 minutes followed by centrifugation (10,000g for 5 minutes) at 37°C. A negative control containing the virus was not centrifuged to determine if the virus degrades throughout the protocol. Supernatant was collected and the pellet was re-suspended in an equal amount of 4°C heat inactive media. Both supernatant and re-suspended pellet were incubated at 4°C for 15 minutes. Then, ELP, KGF-ELP, recombinant KGF, and LDLR3-ELP were added respectively and all samples; supernatant and re-suspended pellet were incubated for 30 minutes at 37°C. Treatments were added to cells for 24 hours with the virus containing NPs. After 24 hours, the old media was discarded, for the A549 cells fresh 37°C serum free media containing DMEM supplemented and 1% AA was added to each well, for the H293 cells fresh 37°C serum media containing DMEM supplemented, 10% FBS, and 1% AA was added to each well. Then, 72 hours later after their respective treatments, the plates were put on ice for five minutes to dissolve fusion proteins, cells were then washed with ice-cold sterile PBS. For visualization purposes fluorescent pictures were taken before analysis of flow cytometry. Nuclei were counterstained with NucBlue (Life Technologies R37605) and fluorescent pictures were taken (20X magnification; bar 200 um) using EVOS fluorescence microscope (Life technologies). Cells were trypsinized using 0.25% trypsin (200 uL). The trypsin reaction was neutralized by an addition of 200 uL of DMEM supplemented with 10% FBS and 1% AA. Solution were transferred into micro-test tubes and cells were pelleted and re-suspend in 250 µL of PBS. Then cells were analyzed using flow cytometry and the normalized fold increase GFP-expressing cells and geometric mean of cells were reported.

Immunoprecipitation Assay

1 µM of biotinylated LDLR3-ELP was incubated with lentiviral vectors at either 4°C or 37 °C for 30 minutes followed by incubation at 4°C for 15 minutes. Samples were incubated with 10 µL of 10 mg/mL dynabeads M-280 Streptavidin (Invitrogen, Carlsbad, CA) at 4°C for 30 minutes. A magnet was used to separate the dynabeads and the supernatant was discarded. Dynabeads were washed three times with sterile 1X PBS. After wash, the

LDLR-3-ELP was eluted using a western blot loading buffer (Cell signaling technology). The eluted samples were then analyzed by western blot using an antibody against the VSV-G protein (1:1000, Sigma-Aldrich cat # V4888) and anti-rabbit IgG HRP-linked antibody (1:5000, Cell Signaling Technology cat # 7074S) to detect the binding of the lentiviral vector. HRP linked Anti-biotin antibody (Cell Signaling Technology cat # 7075P5) was used to detect the biotinylated LDLR3-ELP that was eluted from the dynabeads. Image Studio Lite was used to quantify the western blot bands.

Cells (200,000/well) were seeded in a 6-wells plate and cultured in DMEM supplemented with 10% FBS and 1% AA. They were grown until 30% confluency is reached and were starved for 24 hours and then were treated with nanoparticles containing biotinylated LDLR-3-ELP and lentiviral vectors as described above. At the indicated time points cell lysates were prepared as follows. The cells were put on ice and washed three times with ice cold sterile PBS. The cells were then lysed with radio immune protection assay (RIPA) buffer containing 2X halt protease and phosphatase inhibitors cocktail with 1X ethylene diamine triacetic acid (EDTA) (Thermo scientific cat #78440). Lysates were collected and stored at -80°C . The lysates were c using streptavidin magnetic beads followed by western blot with the VSV-G antibody as described above.

Statistical Analysis

For statistical significance, the p value was calculated for the indicated groups using ANOVA single factor. For the significance of the p values are: ***indicates $P < 0.001$, **indicates $P < 0.05$, and *indicates $P < 0.1$. The reported errors indicated the \pm SD. The power analysis for choosing the sample size was done using the program from the division of Biomathematics/Biostatistics Department of Pediatrics at Columbia University Medical Center (<http://www.biomath.info/power/index.html>). Using typical values (mean difference and standard deviation) of experiments we found out that a sample size of $n=3$ yielded a value of $\alpha = 0.05$ and power = 0.80 where, α : probability (reject H_0 when H_0 is true), and power (reject H_0 when H_1 is true). The variance was similar between groups that were compared statistically.

Acknowledgments

This work was funded in part by NIH grant R21AR068013 (PK) and by Institutional Research Grant number 93-032-16 from the American Cancer Society (PK). We thank Dr. Haura for kindly donating A549, H1650, H23, and H292 cells.

References

1. Nishida K, Smith Z, Rana D, Palmer J, Gallicano GI. Cystic fibrosis: A look into the future of prenatal screening and therapy. Birth defects research Part C, Embryo today : reviews. 2015; 105(1): 73–80.
2. Maude SL, Frey N, Shaw PA, Aplenc R, Barrett DM, Bunin NJ, et al. Chimeric antigen receptor T cells for sustained remissions in leukemia. The New England journal of medicine. 2014; 371(16): 1507–17. [PubMed: 25317870]
3. Bartus RT, Weinberg MS, Samulski RJ. Parkinson's Disease Gene Therapy: Success by Design Meets Failure by Efficacy. Molecular therapy : the journal of the American Society of Gene Therapy. 2014; 22(3):487–97. [PubMed: 24356252]

4. Wu JX, Liu S-H, Nemunaitis JJ, Brunnicardi FC. Liposomal insulin promoter-thymidine kinase gene therapy followed by ganciclovir effectively ablates human pancreatic cancer in mice. *Cancer Letters*. 2015; 359(2):206–10. [PubMed: 25596375]
5. Ko NR, Cheong J, Noronha A, Wilds CJ, Oh JK. Reductively-sheddable cationic nanocarriers for dual chemotherapy and gene therapy with enhanced release. *Colloids and Surfaces B: Biointerfaces*. 2015; 126(0):178–87. [PubMed: 25561416]
6. Kraynyak K, Bodles-Brakhop A, Bagarazzi M. Tapping the Potential of DNA Delivery with Electroporation for Cancer Immunotherapy. *Current Topics in Microbiology and Immunology*: Springer Berlin Heidelberg. 2015:1–24.
7. Cai M, Yang Y. Targeted genome editing tools for disease modeling and gene therapy. *Current gene therapy*. 2014; 14(1):2–9. [PubMed: 24665839]
8. Nasirinezhad F, Gajavelli S, Priddy B, Jergova S, Zadina J, Sagen J. Viral vectors encoding endomorphins and serine histogranin attenuate neuropathic pain symptoms after spinal cord injury in rats. *Molecular pain*. 2015; 11:2.
9. Shearer RF, Saunders DN. Experimental design for stable genetic manipulation in mammalian cell lines: lentivirus and alternatives. *Genes to cells : devoted to molecular & cellular mechanisms*. 2015; 20(1):1–10. [PubMed: 25307957]
10. Frimpong K, Spector SA. Cotransduction of nondividing cells using lentiviral vectors. *Gene therapy*. 2000; 7(18):1562–9. [PubMed: 11021594]
11. Beignon AS, Mollier K, Liard C, Coutant F, Munier S, Riviere J, et al. Lentiviral vector-based prime/boost vaccination against AIDS: pilot study shows protection against Simian immunodeficiency virus SIVmac251 challenge in macaques. *Journal of virology*. 2009; 83(21):10963–74. [PubMed: 19706700]
12. Scaramuzza S, Biasco L, Ripamonti A, Castiello MC, Loperfido M, Draghici E, et al. Preclinical Safety and Efficacy of Human CD34+ Cells Transduced With Lentiviral Vector for the Treatment of Wiskott-Aldrich Syndrome. *Molecular therapy : the journal of the American Society of Gene Therapy*. 2013; 21(1):175–84. [PubMed: 22371846]
13. Craigie R, Bushman FD. HIV DNA integration. *Cold Spring Harbor perspectives in medicine*. 2012; 2(7):a006890. [PubMed: 22762018]
14. Cesani M, Plati T, Lorioli L, Benedicenti F, Redaelli D, Dionisio F, et al. Shedding of clinical-grade lentiviral vectors is not detected in a gene therapy setting. *Gene therapy*. 2015
15. Baum C, Dullmann J, Li Z, Fehse B, Meyer J, Williams DA, et al. Side effects of retroviral gene transfer into hematopoietic stem cells. *Blood*. 2003; 101(6):2099–114. [PubMed: 12511419]
16. Das SK, Menezes ME, Bhatia S, Wang X-Y, Emdad L, Sarkar D, et al. Gene Therapies for Cancer: Strategies, Challenges and Successes. *Journal of cellular physiology*. 2015; 230(2):259–71. [PubMed: 25196387]
17. Lichty BD, Power AT, Stojdl DF, Bell JC. Vesicular stomatitis virus: re-inventing the bullet. *Trends in molecular medicine*. 2004; 10(5):210–6. [PubMed: 15121047]
18. Ge P, Tsao J, Schein S, Green TJ, Luo M, Zhou ZH. Cryo-EM model of the bullet-shaped vesicular stomatitis virus. *Science*. 2010; 327(5966):689–93. [PubMed: 20133572]
19. Cronin J, Zhang XY, Reiser J. Altering the tropism of lentiviral vectors through pseudotyping. *Current gene therapy*. 2005; 5(4):387–98. [PubMed: 16101513]
20. Finkelshtein D, Werman A, Novick D, Barak S, Rubinstein M. LDL receptor and its family members serve as the cellular receptors for vesicular stomatitis virus. *Proceedings of the National Academy of Sciences of the United States of America*. 2013; 110(18):7306–11. [PubMed: 23589850]
21. Han S, Mahato RI, Sung YK, Kim SW. Development of biomaterials for gene therapy. *Molecular therapy : the journal of the American Society of Gene Therapy*. 2000; 2(4):302–17. [PubMed: 11020345]
22. Kowalczyk T, Hnatuszko-Konka K, Gerszberg A, Kononowicz AK. Elastin-like polypeptides as a promising family of genetically-engineered protein based polymers. *World Journal of Microbiology & Biotechnology*. 2014; 30(8):2141–52. [PubMed: 24699809]
23. Rodriguez-Cabello JC, Arias FJ, Rodrigo MA, Girotti A. Elastin-like polypeptides in drug delivery. *Advanced drug delivery reviews*. 2016; 97:85–100. [PubMed: 26705126]

24. Kim JS, Chu HS, Park KI, Won JI, Jang JH. Elastin-like polypeptide matrices for enhancing adeno-associated virus-mediated gene delivery to human neural stem cells. *Gene therapy*. 2012; 19(3): 329–37. [PubMed: 21654823]
25. Dreher MR, Raucher D, Balu N, Michael Colvin O, Ludeman SM, Chilkoti A. Evaluation of an elastin-like polypeptide-doxorubicin conjugate for cancer therapy. *Journal of controlled release : official journal of the Controlled Release Society*. 2003; 91(1–2):31–43. [PubMed: 12932635]
26. Bidwell GL 3rd, Fokt I, Priebe W, Raucher D. Development of elastin-like polypeptide for thermally targeted delivery of doxorubicin. *Biochemical pharmacology*. 2007; 73(5):620–31. [PubMed: 17161827]
27. Koria P, Yagi H, Kitagawa Y, Megeed Z, Nahmias Y, Sheridan R, et al. Self-assembling elastin-like peptides growth factor chimeric nanoparticles for the treatment of chronic wounds. *Proceedings of the National Academy of Sciences of the United States of America*. 2011; 108(3):1034–9. [PubMed: 21193639]
28. Trabbic Carlson K, Meyer DE, Liu L, Piervincenzi R, Nath N, LaBean T, et al. Effect of protein fusion on the transition temperature of an environmentally responsive elastin like polypeptide: a role for surface hydrophobicity? *Protein Engineering Design and Selection*. 2004; 17(1):57–66.
29. Urry DW. Physical Chemistry of Biological Free Energy Transduction As Demonstrated by Elastic Protein-Based Polymers. *The Journal of Physical Chemistry B*. 1997; 101(51):11007–28.
30. Meyer DE, Chilkoti A. Purification of recombinant proteins by fusion with thermally-responsive polypeptides. *Nature biotechnology*. 1999; 17(11):1112–5.
31. McCarthy B, Yuan Y, Koria P. Elastin-like-polypeptide based fusion proteins for osteogenic factor delivery in bone healing. *Biotechnology progress*. 2016; 32(4):1029–37. [PubMed: 27038196]
32. Johnson T, Koria P. Expression and Purification of Neurotrophin-Elastin-Like Peptide Fusion Proteins for Neural Regeneration. *BioDrugs: clinical immunotherapeutics, biopharmaceuticals and gene therapy*. 2016; 30(2):117–27.
33. Iglesias R, Koria P. Leveraging growth factor induced macropinocytosis for targeted treatment of lung cancer. *Medical oncology (Northwood, London, England)*. 2015; 32(12):259.
34. Lopes CD, Goncalves NP, Gomes CP, Saraiva MJ, Pego AP. BDNF gene delivery mediated by neuron-targeted nanoparticles is neuroprotective in peripheral nerve injury. *Biomaterials*. 2017; 121:83–96. [PubMed: 28081461]
35. Chen Y, Xu M, Guo Y, Tu K, Wu W, Wang J, et al. Targeted chimera delivery to ovarian cancer cells by heterogeneous gold magnetic nanoparticle. *Nanotechnology*. 2017; 28(2):025101. [PubMed: 27906685]
36. Chorny M, Fishbein I, Tengood JE, Adamo RF, Alferiev IS, Levy RJ. Site-specific gene delivery to stented arteries using magnetically guided zinc oleate-based nanoparticles loaded with adenoviral vectors. *FASEB J*. 2013; 27(6):2198–206. [PubMed: 23407712]
37. Wenzel D, Rieck S, Vosen S, Mykhaylyk O, Trueck C, Eberbeck D, et al. Identification of magnetic nanoparticles for combined positioning and lentiviral transduction of endothelial cells. *Pharm Res*. 2012; 29(5):1242–54. [PubMed: 22231984]
38. Choi JW, Park JW, Na Y, Jung SJ, Hwang JK, Choi D, et al. Using a magnetic field to redirect an oncolytic adenovirus complexed with iron oxide augments gene therapy efficacy. *Biomaterials*. 2015; 65:163–74. [PubMed: 26164117]
39. Meyer DE, Chilkoti A. Genetically encoded synthesis of protein-based polymers with precisely specified molecular weight and sequence by recursive directional ligation: examples from the elastin-like polypeptide system. *Biomacromolecules*. 2002; 3(2):357–67. [PubMed: 11888323]

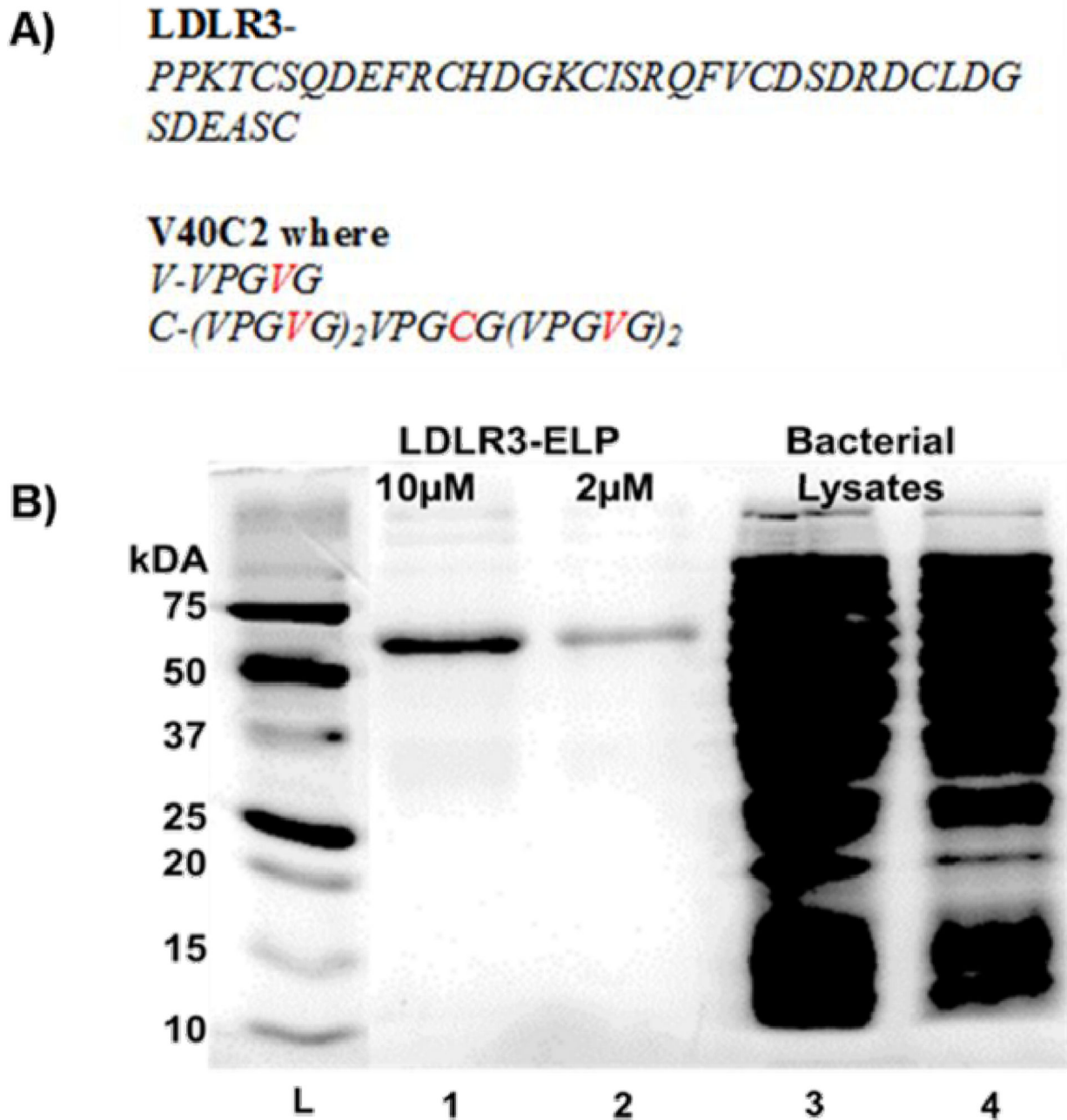


Figure 1. Fusion protein comprising of the viral envelope binding domain (VBD) and elastin like polypeptide (ELP) was successfully expressed and purified using inverse temperature cycling (ITC)

A) Sequence of LDLR3-ELP and ELP. **B)** The bacterial lysate and purified LDLR3-ELP fusion protein was run on a SDS-PAGE gel and stained with simply safe blue stain for total protein. Lanes: L=ladder, lanes 1 and 2, 10 μM and 2 μM of purified LDLR3-ELP fusion respectively, and lanes 3 and 4 bacterial lysates. SDS, sodium dodecyl sulfate; PAGE, polyacrylamide gel electrophoresis. Red color represents guest residues.

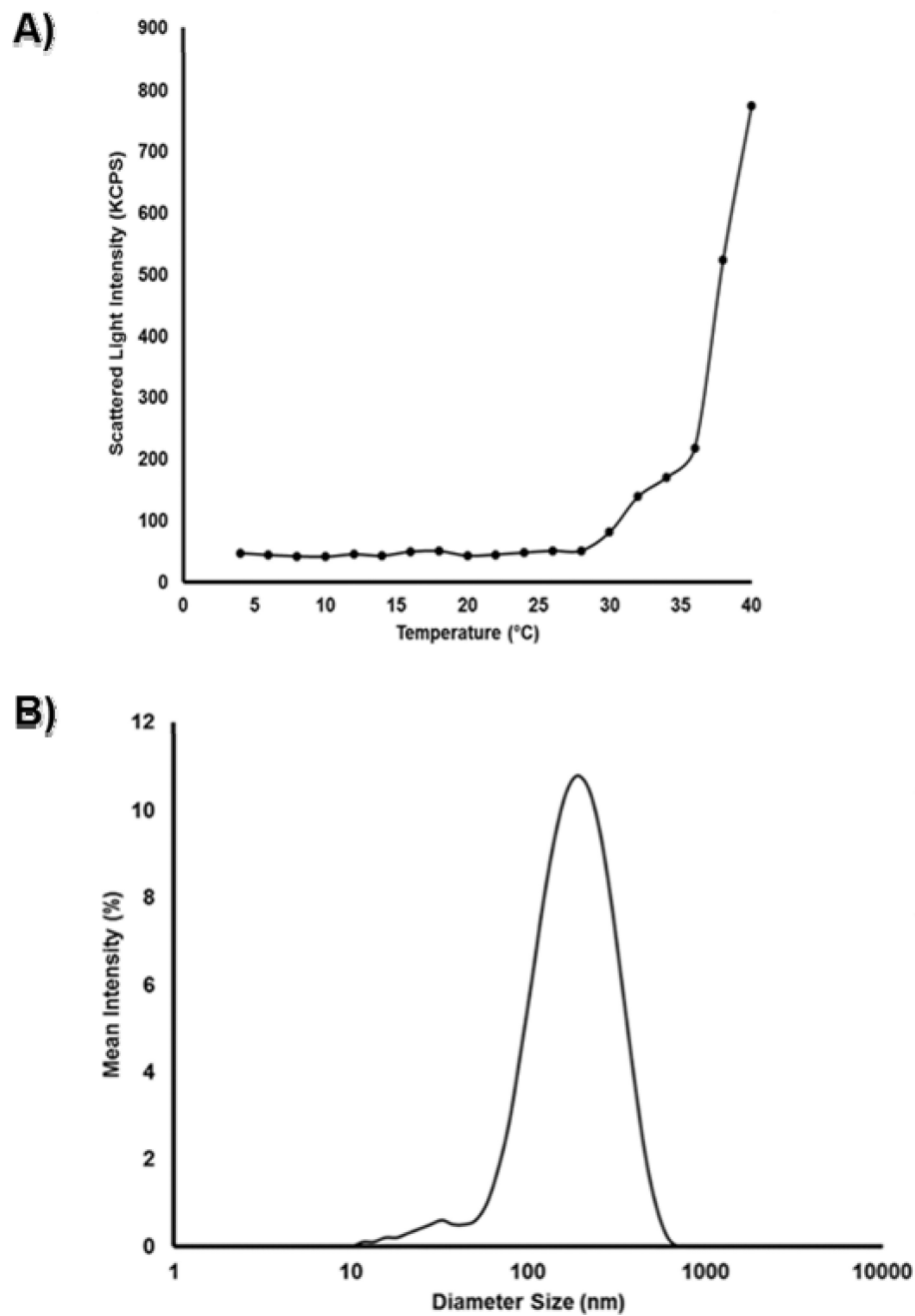


Figure 2. LDLR3-ELP maintains the phase transition property and self assembles into nanoparticles

A) LDLR3-ELP transitions around 30°C. The transition temperature of 2 μ M LDLR3-ELP was taken using dynamic light scattering (DLS). **B)** LDLR3-ELP size is in the nanometer range at physiological temperature. The size distribution of LDLR3-ELP by intensity is 204 nm at 37°C. Samples were dissolved in 1X sterile PBS.

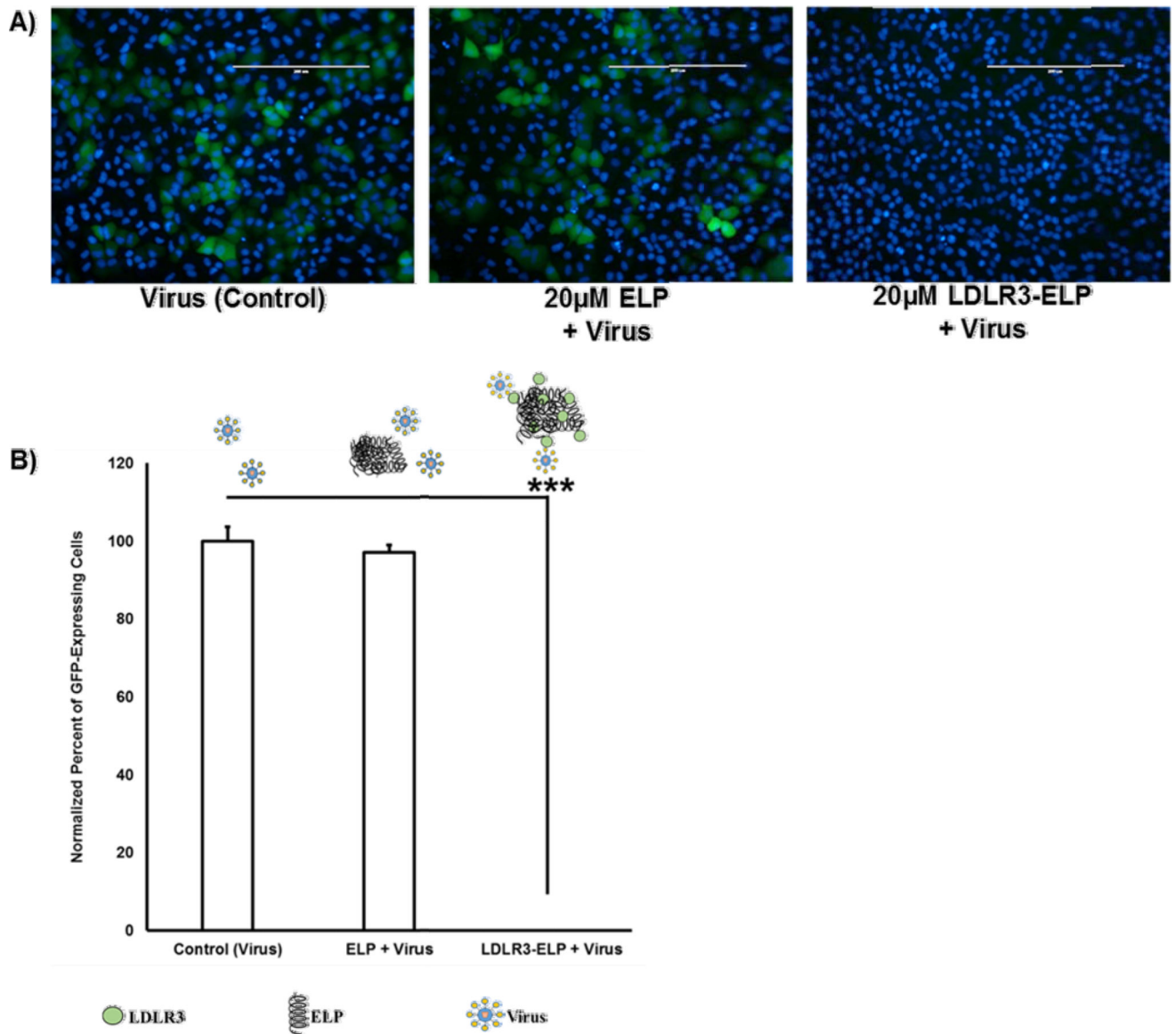
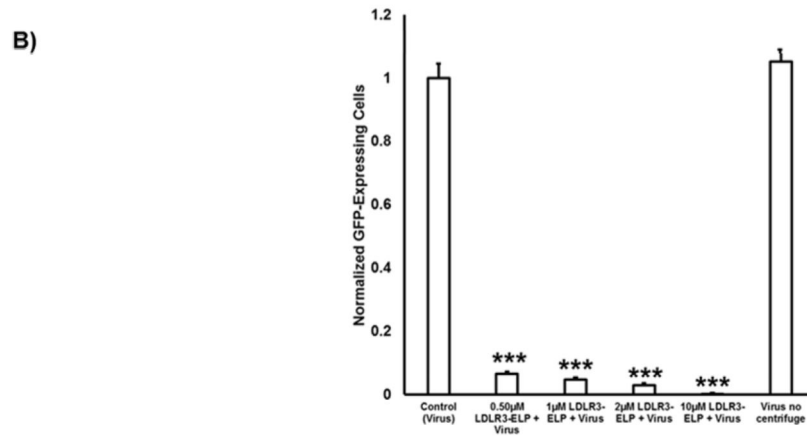
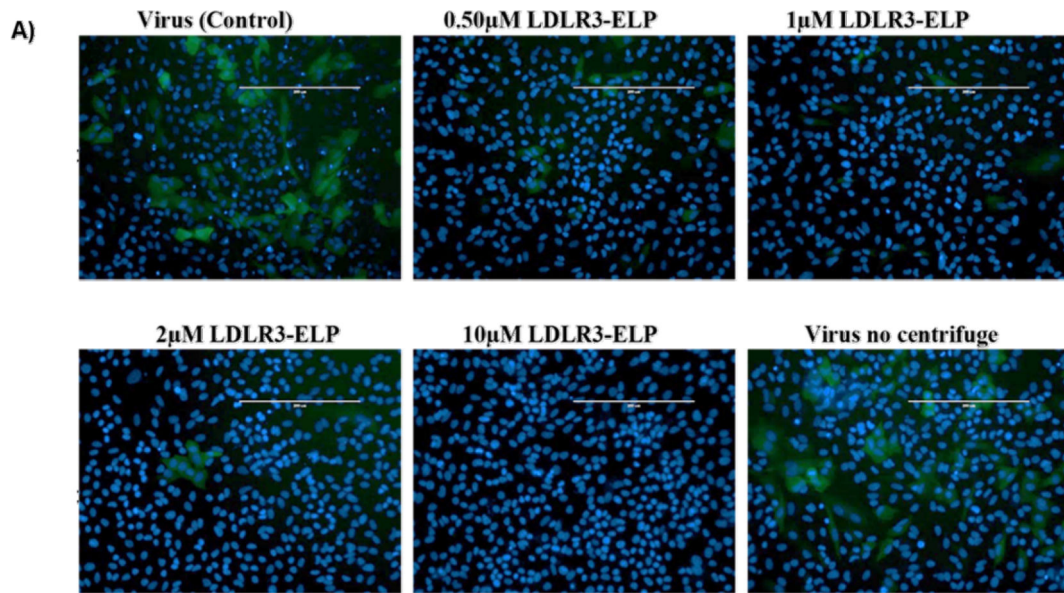


Figure 3. LDLR3-ELP inhibits VSV-G pseudotyped lentiviral vector infectivity

A) GFP expression in A549 cells, 20 μ M ELP and 20 μ M LDLR3-ELP, n=3. **B)** Average \pm SD of the normalized GFP expression. A549 cells were starved for 24 hours. The lentiviral vectors were incubated with the NPs prior to cell treatment. Then the cells were incubated for 24 hours with the lentiviral vectors containing NPs. After 24 hours, the old media was discarded and fresh serum free 37°C media was added to each well. Then, 72 hours later, the transduction efficiency was quantified using flow cytometry. Treatments were normalized to control (virus). These experiments were repeated two more times with triplicates.

***indicates $P < 0.001$ when compared to control (virus). Error bars represent \pm SD.



c) IP: Streptavidin coated dynabeads

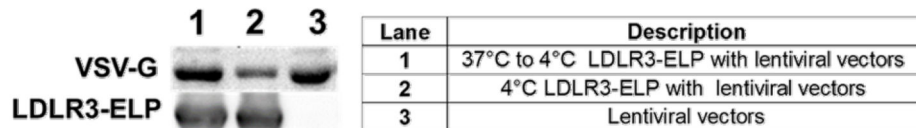


Figure 4. LDLR3-ELP binds to the lentiviral vector and inhibits the VSV-G pseudotyped lentiviral vector infectivity in A549 cells at different concentrations

A) GFP expression in A549 cells, LDLR3 at 0.50 μM, 1 μM, 2 μM, and 10 μM B) Average ± SD of the normalized GFP expression of supernatant. A549 cells were starved for 24 hours and cells were treated for 24 hours with the lentiviral vector containing NPs as described in materials and methods. After 24 hours, the old media was discarded, and fresh 37°C serum free media was added to each well. Then, 72 hours later, the transduction efficiency was quantified using flow cytometry. Treatments were normalized to control (virus). All the treatments except with “virus no centrifuge” went through the centrifugation process. (C) LDLR-3-ELP has three times the binding affinity at 37°C compared to 4°C. 1 μM of

biotinylated LDLR3-ELP was incubated with lentiviral vectors either at 4°C or 37°C for 30 minutes, followed by a 15 minute incubation at 4°C. Binding of the lentiviral vector to LDLR-3-ELP was assessed by immunoprecipitation assay as described in materials and methods. The viral binding was assessed by western blot for the VSV-G protein. Since the lentiviral vectors were not biotinylated, there is no band in lane three of LDLR3-ELP. Image Studio Lite was used to quantify the western blot bands. All experiments were repeated two more times with triplicates. ***indicates $P < 0.001$ when compared to control (virus). Error bars represent \pm SD.

Author Manuscript

Author Manuscript

Author Manuscript

Author Manuscript

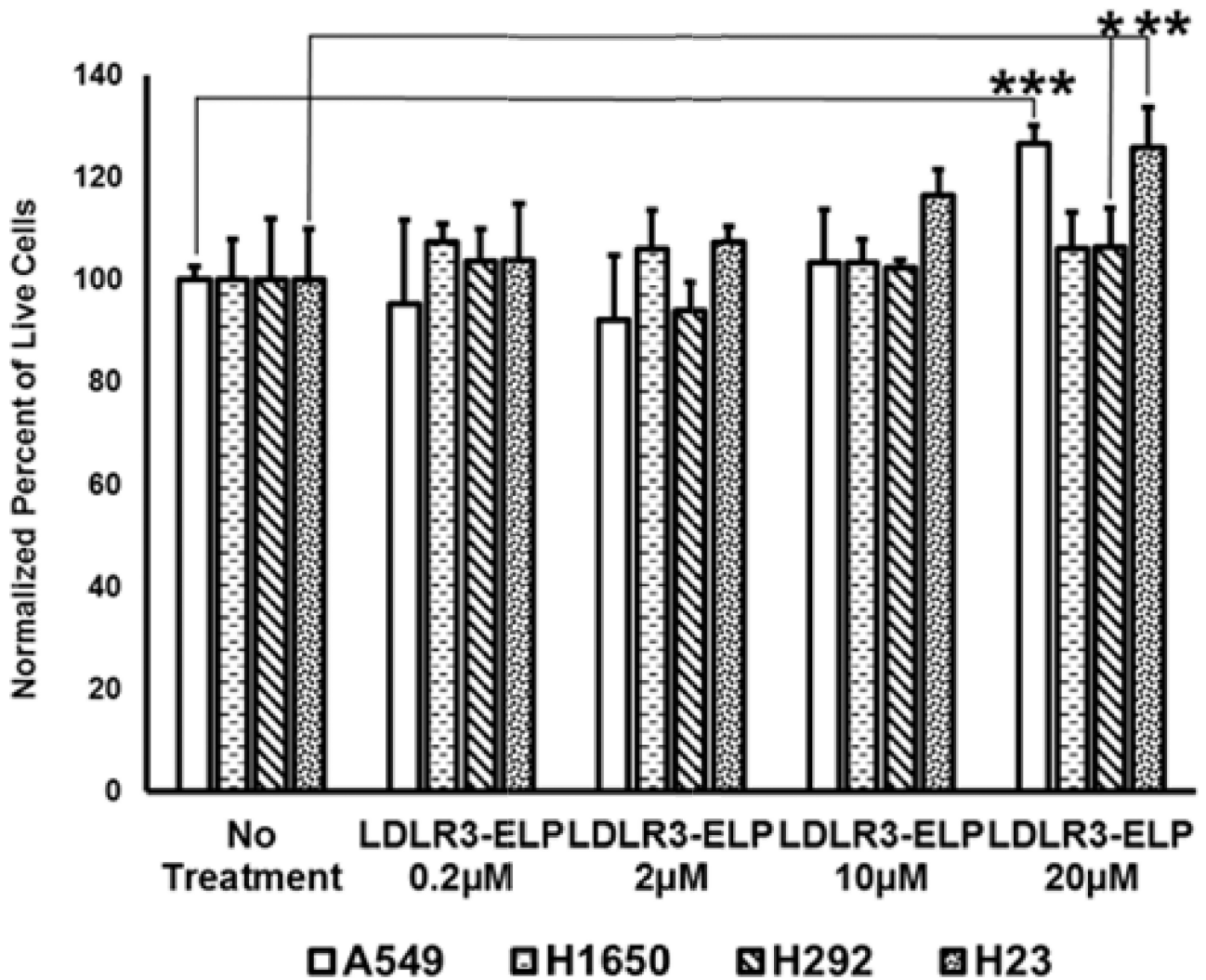


Figure 5. LDLR3-ELP does not induce cell death

A549, H1650, H292, and H23 cells were starved for 24 hours then were treated in serum free media with the indicated treatments 0.2 µM, 2 µM, 10 µM and 20 µM LDLR3-ELP for 48 hours. After 48 hours, a MTT assay was performed and a spectrophotometer was used to read the absorbance at 570 nm. Treatments were normalized to control (no treatment). These experiments were repeated two more times with triplicates. ***indicates P<0.001, **indicates P<0.05, and *indicates P<0.1 when compared to control (no treatment). Error bars represent ± SD.

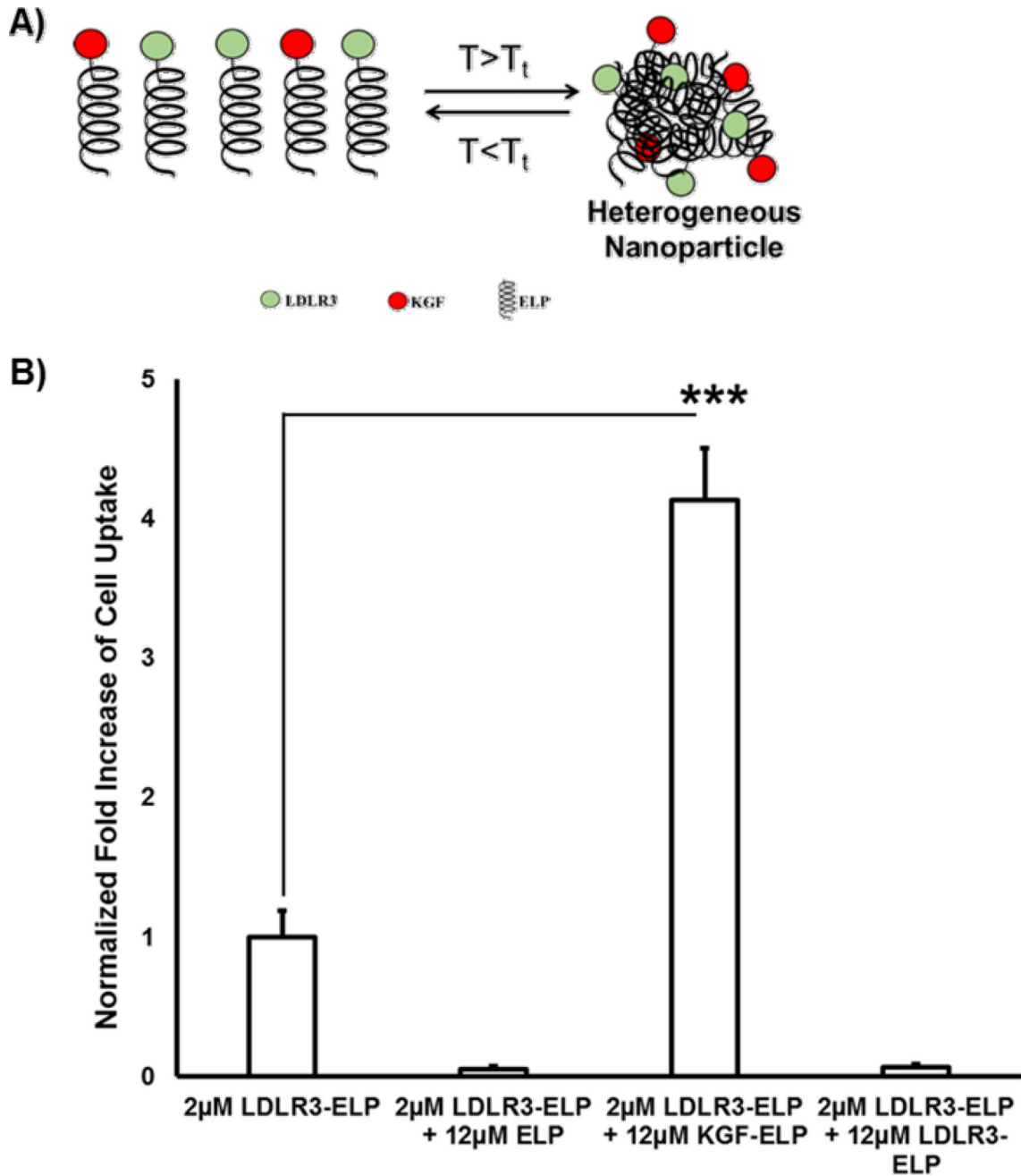


Figure 6. Targeted internalization of LDLR3-ELP using growth factors in high growth factor receptor expressing cells

A) Schematic of heterogeneous nanoparticle. **B)** Average \pm SD of the normalized fold increase of cell uptake. A549 cells were starved for 24 hours then were treated in serum free media with the indicated treatments fluorescein-labeled 2 μ M LDLR3-ELP and combination of fluorescein-labeled 2 μ M LDLR3-ELP and ELP and KGF-ELP, and LDLR3-ELP for 48 hours. Lentiviral vectors were not added in this experiment. After 48 hours, flow cytometry was used to quantify the data. Before analysis, trypan blue was used in each sample suspension to capture only the internalized labeled fusion proteins and not the ones that are bound to the periphery of the cells. These experiments were repeated two more times with

triplicates. ***indicates $P < 0.001$ when compared to control (2 μM LDLR3-ELP). Error bars represent \pm SD.

Author Manuscript

Author Manuscript

Author Manuscript

Author Manuscript

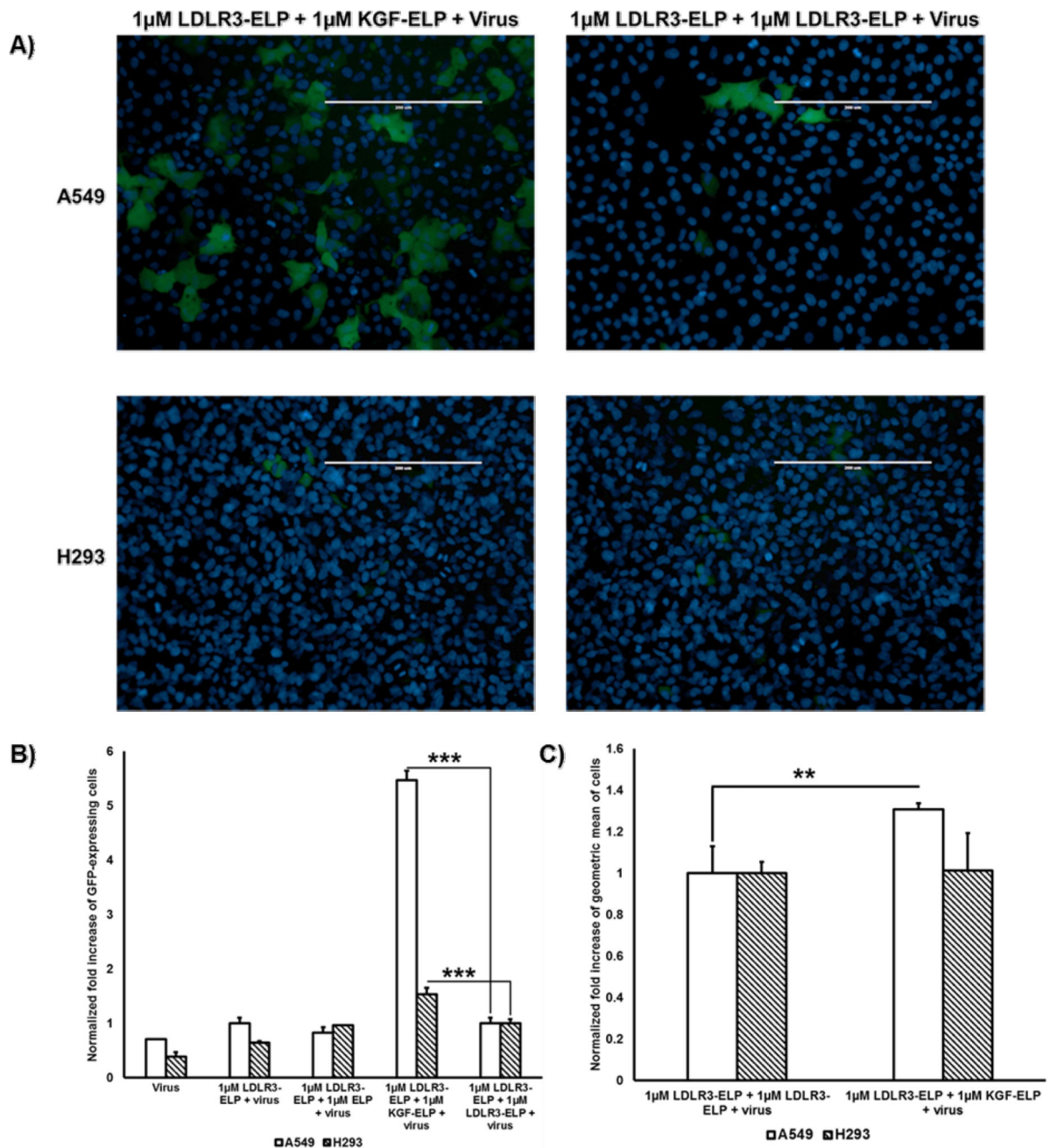


Figure 7. Heterogeneous nanoparticles comprising of LDLR-3-ELP and KGF-ELP result in targeted delivery of the gene in high growth factor receptor expressing cells

A) GFP expression in A549 cells and H293 cells. **B)** Average \pm SD of the normalized GFP expression of pellet. **C)** Average \pm SD of the normalized geometric mean of cells. Cells were starved for 24 hours and treatment started when their confluency reached 30%. The cells were treated with the indicated NP formulations as described in materials and methods. 72 hours after treatment the transduction efficiency was quantified using flow cytometry. Treatments were normalized to control (1 μ M LDLR3-ELP + 1 μ M LDLR3-ELP + Virus) for each cell type to account for differences in transduction that may arise due to different cell types. These experiments were repeated two more times with triplicates. ***indicates

P<0.001 and **indicates P<0.05 when compared to control (1 μ M LDLR3-ELP + 1 μ M LDLR3-ELP + Virus). Error bars represent \pm SD.

Author Manuscript

Author Manuscript

Author Manuscript

Author Manuscript

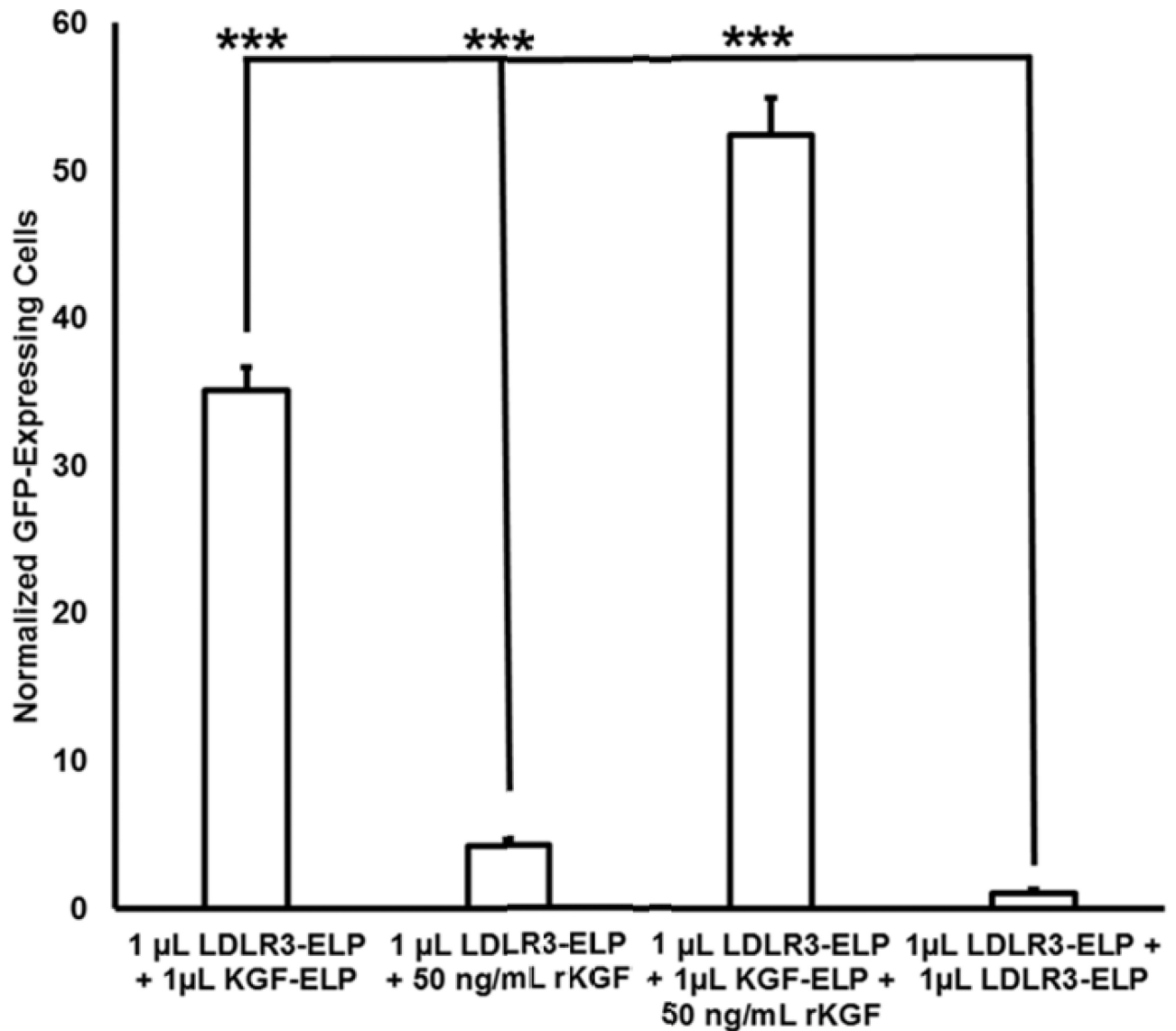


Figure 8. Recombinant KGF increased the transduction efficiency blocked by LDLR3-ELP
 A549 cells were starved for 24 hours and then treated with lentiviral vector bound to either LDLR-3-ELP homogeneous or KGF-ELP LDLR3-ELP heterogeneous nanoparticles in the presence or absence of recombinant KGF (rKGF). After 24 hours, the old media was discarded, and fresh 37°C serum free media was added to each well. 72 hours later, the transduction efficiency was quantified using flow cytometry. Treatments were normalized to control (1 μ M LDLR3-ELP + 1 μ M LDLR3-ELP + Virus). These experiments were repeated two more times with triplicates. ***indicates $P < 0.001$ when compared to control (1 μ M LDLR3-ELP + 1 μ M LDLR3-ELP). Error bars represent \pm SD.

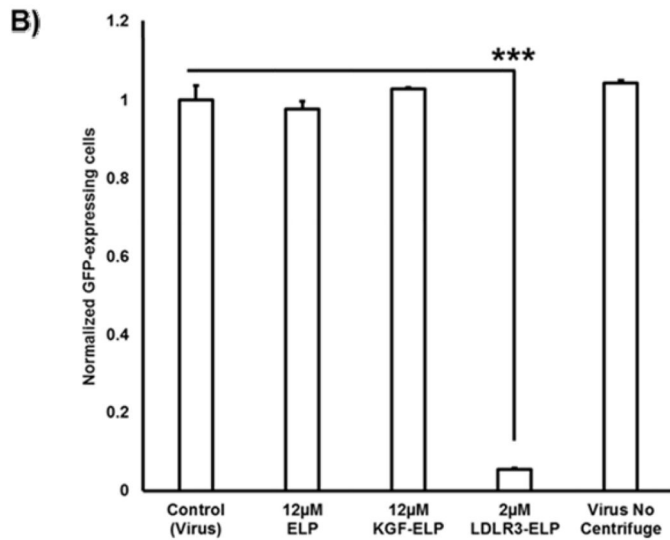
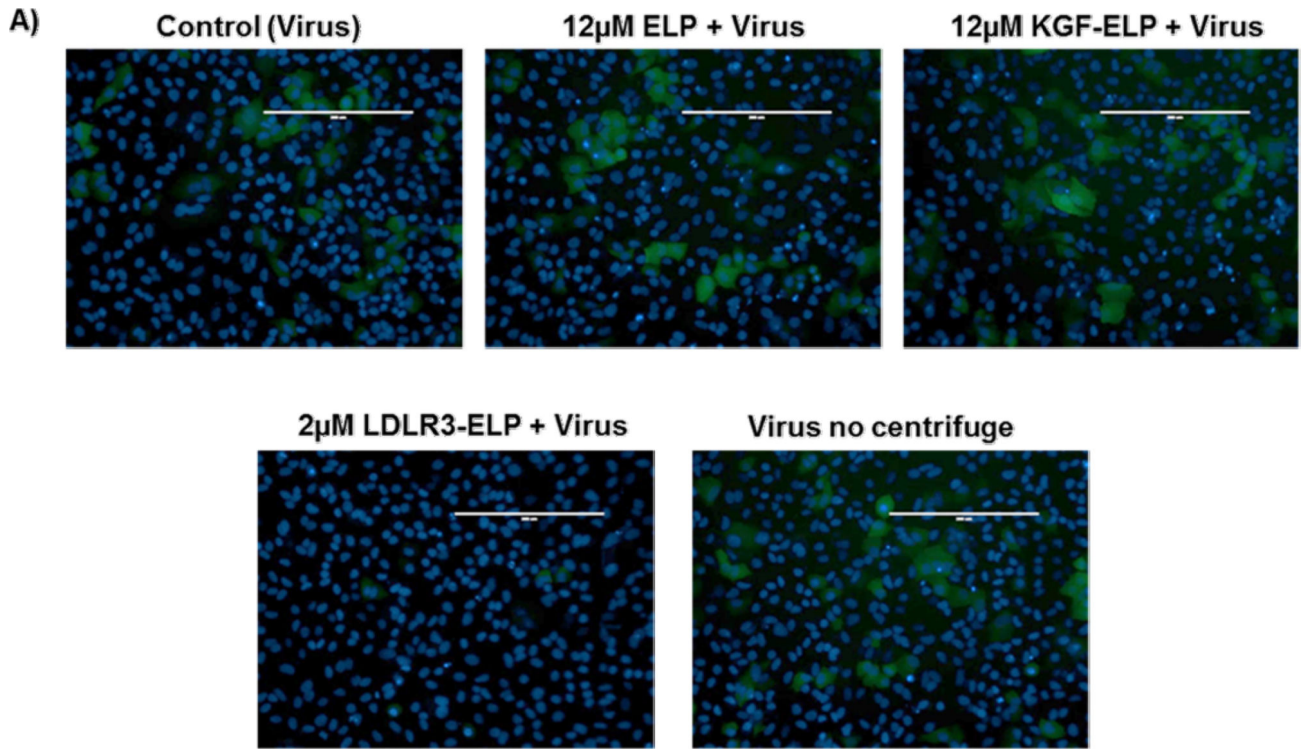


Figure 9. ELP and KGF-ELP do not bind to the VSV-G pseudotyped lentiviral vector
A) GFP expression in A549 cells. **B)** Average \pm SD of the normalized GFP expression of supernatant. A549 cells were starved for 24 hours. A binding assay was performed and cells were treated with the supernatant. Cells were treated for 24 hours with the lentiviral vector containing 12 μ M ELP, 12 μ M KGF-ELP, and 2 μ M LDLR3-ELP were added respectively. After 24 hours, the old media was discarded, and fresh 37°C serum free media was added to each well. Then, 72 hours later, the transduction efficiency was quantified using flow cytometry. Treatments were normalized to control (virus). These experiments were repeated

two more times with triplicates. ***indicates $P < 0.001$ when compared to control (virus). Error bars represent \pm SD.

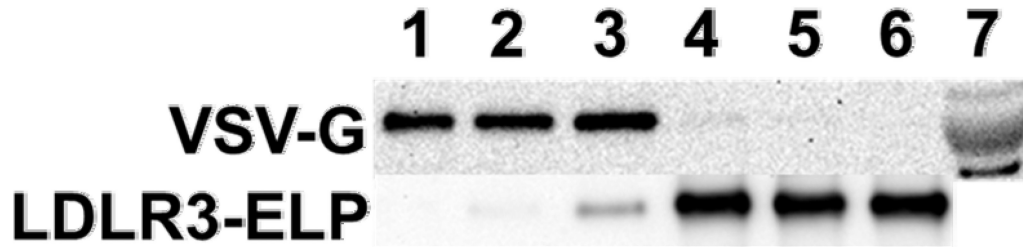
Author Manuscript

Author Manuscript

Author Manuscript

Author Manuscript

IP: Streptavidin coated dynabeads



Lane	Description
1	LDLR3-ELP + KGF-ELP 24 hrs supernatant
2	LDLR3-ELP + KGF-ELP 48 hrs supernatant
3	LDLR3-ELP + KGF-ELP 72 hrs supernatant
4	LDLR3-ELP + KGF-ELP 72 hrs dynabeads
5	LDLR3-ELP + KGF-ELP 48 hrs dynabeads
6	LDLR3-ELP + KGF-ELP 24 hrs dynabeads
7	Lentiviral vectors

Figure 10. Lentiviral vector is released from LDLR3-ELP after internalization by cells
 A549 were starved for 24 hours then were treated in serum free media with the indicated treatments. Cells were treated for 24 hours with the lentiviral vector containing nanoparticles that consisted of 1 μ M of biotinylated LDLR3-ELP and 1 μ M KGF-ELP. At the indicated time points, cells were put on ice for five minutes followed by three ice cold washes in PBS. The cells were lysed with radio immune protection assay (RIPA) buffer containing 2X halt protease and phosphatase inhibitors cocktail with 1X ethylene diamine triacetic acid (EDTA). The lysates were immunoprecipitated using streptavidin conjugated magnetic beads (dynabeads). Then a magnetic bar was used to separate the beads from the supernatant. Following a few washes, the immunoprecipitated complexes (dynabeads) and the supernatant were analyzed for the presence of virus using western blots. Anti VSV-G antibody was used to detect the lentiviral vector.